AMERICAN SOCIETY FOR MICROBIOLOGY | Infection and Immunity®

HOST RESPONSE AND INFLAMMATION

Temporal Role for MyD88 in a Model of *Brucella*-Induced Arthritis and Musculoskeletal Inflammation

Carolyn A. Lacey,[a,b] William J. Mitchell,[a] Charles R. Brown,[a] Jerod A. Skyberg[a,b]

Department of Veterinary Pathobiology, College of Veterinary Medicine, University of Missouri, Columbia, Missouri, USA[a]; Laboratory for Infectious Disease Research, University of Missouri, Columbia, Missouri, USA[b]

ABSTRACT *Brucella* spp. are facultative intracellular Gram-negative bacteria that cause the zoonotic disease brucellosis, one of the most common global zoonoses. Osteomyelitis, arthritis, and musculoskeletal inflammation are common focal complications of brucellosis in humans; however, wild-type (WT) mice infected systemically with conventional doses of *Brucella* do not develop these complications. Here we report C57BL/6 WT mice infected via the footpad with 10^3 to 10^6 CFU of *Brucella* spp. display neutrophil and monocyte infiltration of the joint space and surrounding musculoskeletal tissue. Joint inflammation is detectable as early as 1 day postinfection and peaks 1 to 2 weeks later, after which WT mice are able to slowly resolve inflammation. B and T cells were dispensable for the onset of swelling but required for resolution of joint inflammation and infection. At early time points, MyD88$^{-/-}$ mice display decreased joint inflammation, swelling, and proinflammatory cytokine levels relative to WT mice. Subsequently, swelling of MyD88$^{-/-}$ joints surpassed WT joint swelling, and resolution of joint inflammation was prolonged. Joint bacterial loads in MyD88$^{-/-}$ mice were significantly greater than those in WT mice by day 3 postinfection and at all time points thereafter. In addition, MyD88$^{-/-}$ joint inflammatory cytokine levels on day 3 and beyond were similar to WT levels. Collectively these data demonstrate MyD88 signaling mediates early inflammatory responses in the joint but also contributes to subsequent clearance of *Brucella* and resolution of inflammation. This work also establishes a mouse model for studying *Brucella*-induced arthritis, musculoskeletal complications, and systemic responses, which will lead to a better understanding of focal complications of brucellosis.

KEYWORDS arthritis, osteomyelitis, *Brucella*, brucellosis, MyD88, musculoskeletal

Received 6 December 2016 **Returned for modification** 29 December 2016 **Accepted** 5 January 2017

Accepted manuscript posted online 9 January 2017

Citation Lacey CA, Mitchell WJ, Brown CR, Skyberg JA. 2017. Temporal role for MyD88 in a model of *Brucella*-induced arthritis and musculoskeletal inflammation. Infect Immun 85:e00961-16. https://doi.org/10.1128/IAI.00961-16.

Editor Guy H. Palmer, Washington State University

Address correspondence to Jerod A. Skyberg, skybergj@missouri.edu.

Brucella spp. infect over 500,000 individuals each year, making brucellosis one of the most common global zoonoses (1). The most prevalent species that infect humans are *Brucella melitensis*, *Brucella abortus*, and *Brucella suis* (2). Transmission to humans typically occurs through the consumption of unpasteurized dairy products or via aerosol following contact with contaminated meat products (3, 4). Although vaccination of livestock has reduced disease incidence, no licensed human vaccine is available, and brucellosis has recently been designated a neglected zoonotic disease by the World Health Organization (5, 6). Osteoarticular and musculoskeletal inflammation are the most common focal complications of human brucellosis and occur in 40 to 80% of *Brucella*-infected patients (7, 8). This arthritis is thought to arise from the hematogenous spread of *Brucella* to the joints, as viable brucellae can be found within the synovial fluid of infected patients (9, 10). Arthritis can manifest as peripheral arthritis, sacroiliitis, and spondylitis, which are most common in children, young adults and older adults, respectively (7, 8, 11, 12). Inflammation of the joint synovium is prevalent in infected individuals, with polymorphonuclear and mononuclear leukocytes found in and around synovial tissue (13). *Brucella*-induced arthritis is commonly treated with antibiotics;

however, resolution of arthritis is often protracted, and the disease can relapse (8, 14). Untreated articular brucellosis can result in synovial rupture or bone destruction, potentially causing permanent disability (12, 15, 16).

Mechanisms underlying arthritic responses induced by *Brucella* have been hindered by the lack of relevant mouse models, as wild-type (WT) mice infected with conventional doses (10^4 to 10^6 CFU) by systemic routes do not develop joint inflammation (9, 17). One study showed that BALB/c mice infected intraperitoneally (i.p.) with 1×10^7 CFU of *B. melitensis* developed arthritis at 26 weeks postinfection (18). Additionally, we have previously reported that i.p. *Brucella* infection of gamma interferon (IFN-γ)-deficient mice resulted in arthritis of ankle joints as early as 15 days postinfection. Arthritis in this model was dependent on CXCR2 and interleukin-1 receptor (IL-1R), but adaptive immune cells were not required for the induction of inflammation (9, 17). We suspected that IFN-γ deficiency allowed for the hematogenous spread of *Brucella*, resulting in infection and inflammation of the joint (9). Other mouse models of infectious arthritis have utilized footpad inoculation to localize pathogens, such as *Borrelia burgdorferi*, chikungunya virus, and *Candida albicans*, to the joint and surrounding tissue to induce inflammation (19–21) Here we describe a model of *Brucella*-induced arthritis that is applicable in WT mice. Infection of the articular space and surrounding tissue is achieved by injecting *Brucella* adjacent to ankle joints, via footpad inoculation.

Myeloid differentiation factor 88 (MyD88) is an adaptor protein that relays Toll-like receptor (TLR), IL-1R, and IL-18R signaling (22, 23). Once activated, most TLRs signal through MyD88 to induce cytokine production (24). This signaling can result in arthritis and osteoclastogenesis in murine models of bacterium-induced focal complications (25–27). Host cells reportedly recognize *Brucella* through TLR2, TLR4, TLR6, and TLR9 (28–32). To determine if MyD88 signaling is important for *Brucella*-induced arthritis, we investigated joint inflammatory responses in MyD88$^{-/-}$ mice following footpad infection with *Brucella*. We show MyD88 regulates early arthritis development but is also required to control bacterial burden and resolve inflammation at later stages of infection.

RESULTS

***Brucella* infection of the footpad results in arthritis and musculoskeletal inflammation in wild-type mice.** The systemic spread of *Brucella* to the joints is thought to induce arthritis and musculoskeletal inflammation (9). Thus, we hypothesized that delivering *Brucella* adjacent to the joint would allow for bacterial colonization and subsequent arthritis. Therefore, we infected C57BL/6 wild-type (WT) mice in the rear footpads with 1×10^6 CFU of *B. melitensis* 16M. Hematoxylin and eosin (H&E) staining was conducted on mock-infected mice at day 3, and *Brucella*-infected mice at days 1, 3, 7, 14, and 28 postinfection (Fig. 1A to F). All footpad-infected mice exhibited signs of arthritis and musculoskeletal inflammation in the joint and surrounding muscle and soft tissues relative to mock-infected mice (Fig. 1B to F). *Brucella*-infected C57BL/6 mice demonstrated moderate to focally extensive areas of inflammation and large numbers of neutrophils, including neutrophils in the joint space, 1 day after infection (Fig. 1B). Joint arthritis and musculoskeletal inflammation peaked from days 3 to 14, presenting with severe large confluent areas of inflammation (neutrophils, macrophages, and fibrin in the joint space) (Fig. 1C to E). Inflammation began to resolve by day 28, with moderate to severe pathology with focally extensive areas of inflammation, including macrophages, fibrin, and few neutrophils in the joint space (Fig. 1F).

Footpad inoculation of mice with *B. melitensis*, *B. suis*, or *B. abortus* results in dose-dependent joint swelling, arthritis, and musculoskeletal inflammation. To determine if footpad inoculation with a lower dose or other *Brucella* species pathogenic in humans could also induce arthritis, we injected 1×10^5 cells of *B. melitensis* 16M, *B. suis* 1330, or *B. abortus* 2308 into the footpads of C57BL/6 WT mice. Joint swelling was also measured as it is a characteristic manifestation of *Brucella*-induced arthritis and musculoskeletal inflammation (9, 17). Relative to *B. melitensis*-infected mice, swelling of joints was slightly but significantly greater in *B. abortus*-infected mice on day 2 and in

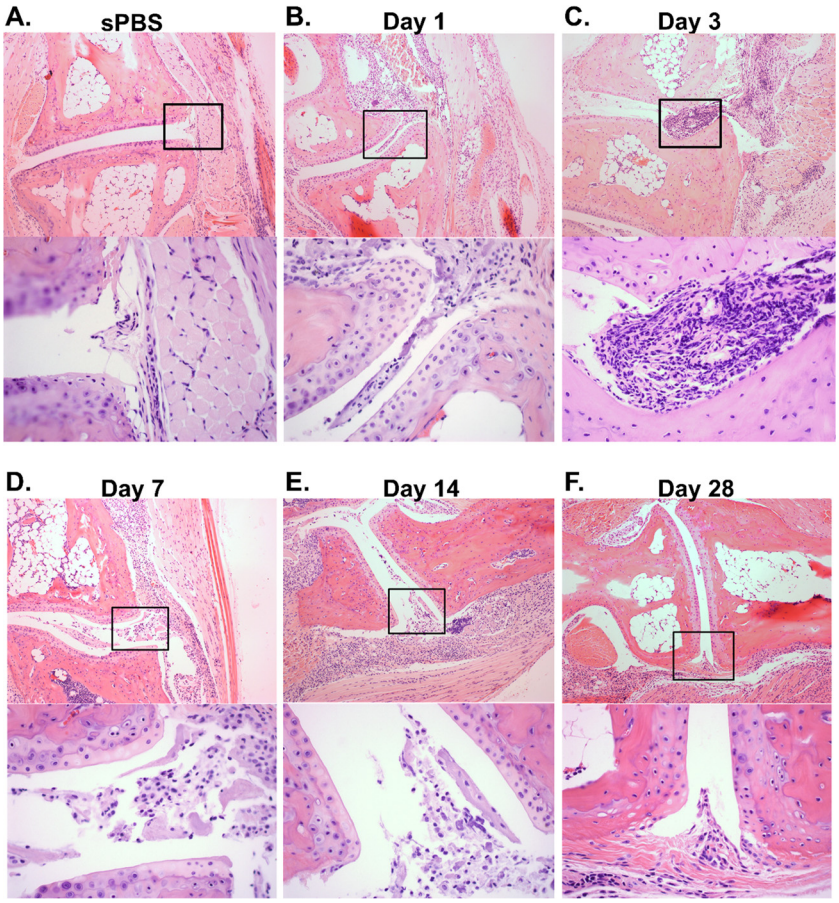

FIG 1 WT mice develop arthritis and musculoskeletal inflammation following footpad infection. C57BL/6 WT mice were either mock infected in each rear footpad with sterile PBS (sPBS) or infected with 1×10^6 CFU of *B. melitensis* 16M. Mock-infected mice were euthanized at day 3 (A), and *B. melitensis*-infected mice were euthanized at days 1 (B), 3 (C), 7 (D), 14 (E), and 28 (F) postinfection. H&E staining was conducted on mouse joints. Representative images (100×) from mock-treated and infected mice are depicted. Amplified boxed regions (400×) showing inflammation within the joint space of *B. melitensis*-infected mice are displayed beneath the 100× image at each time point. Images are representative of joints from 4 to 5 mice per time point from one kinetic experiment. Similar pathology was observed at the day 3 and day 28 time points in 2 to 3 additional experiments.

B. suis-infected mice on days 2 and 11. However, all *Brucella* species displayed similar swelling kinetics and induced robust swelling of mouse ankles by day 2 postinfection (Fig. 2A). Additionally, we investigated if *B. melitensis* 16M at a dose of 1×10^3 or 1×10^4 CFU could induce inflammation via footpad infection (Fig. 2A and C). Although ankle swelling was evident, it was slightly delayed in mice infected with a dose of 1×10^4 CFU compared to mice infected with 1×10^5 CFU of *B. melitensis* (Fig. 2A). Similarly, mice infected with 1×10^3 CFU of *B. melitensis* also developed joint swelling, while no apparent swelling was found in mice mock infected with sterile phosphate-buffered saline (sPBS) (Fig. 2C). Additionally, bacterial loads in joint homogenates were similar between mice infected with 1×10^5 CFU of *B. abortus*, *B. suis*, or *B. melitensis* 14 days after infection (Fig. 2B). To determine if *Brucella* was able to colonize systemic tissues in this model, splenic bacterial loads were measured, and *B. melitensis*, *B. abortus*, and *B. suis* were all found to similarly colonize the spleen following footpad inoculation with 1×10^5 CFU (Fig. 2B). Bacterial colonization was also detected in the joints and spleens of mice infected with 1×10^3 or 1×10^4 CFU of *B. melitensis* (Fig. 2B and D). On day 14 postinfection, histology was conducted on joint sections from mock-infected mice, along with mice infected with 1×10^3 to 1×10^5 CFU of *B. melitensis* or with 1×10^5 CFU of *B. suis* or *B. abortus* (Fig. 2E to J). All *Brucella*-infected mice (Fig. 2F to J)

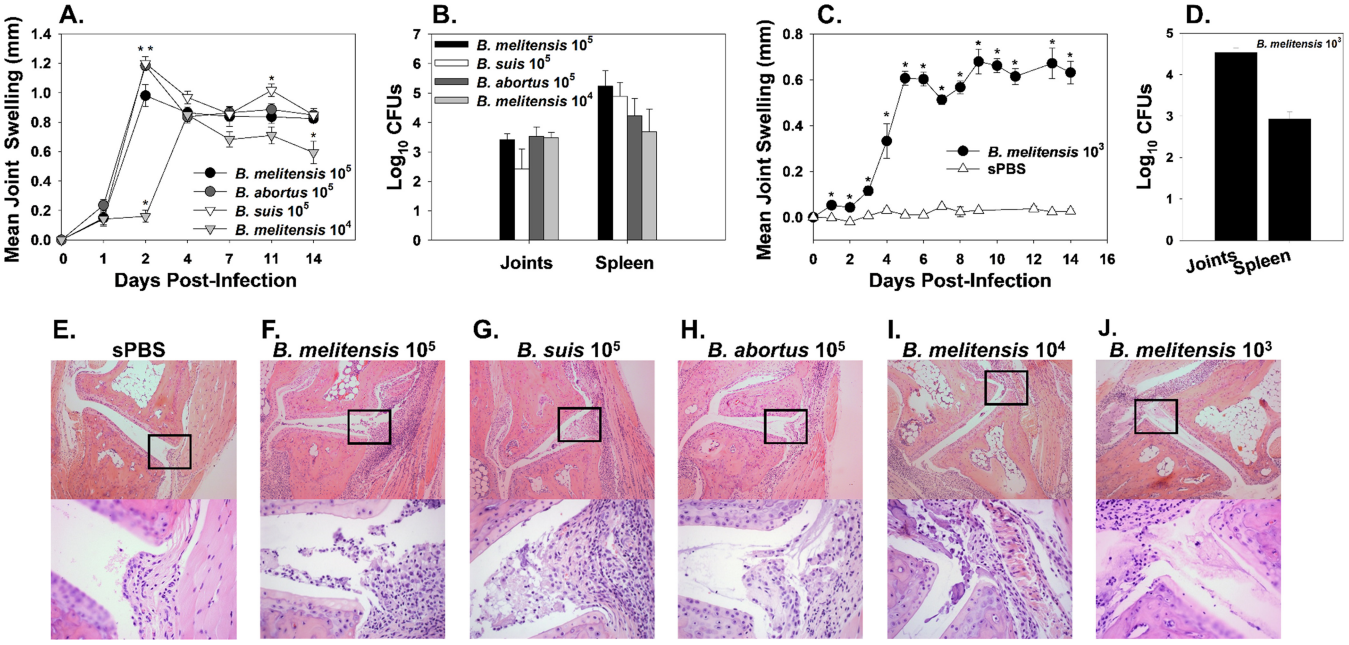

FIG 2 WT mice infected via the footpad with *B. melitensis*, *B. abortus*, or *B. suis* develop arthritis and musculoskeletal inflammation. C57BL/6 WT mice were infected in each rear footpad with 1×10^5 CFU of *Brucella* spp., 1×10^4 CFU of *B. melitensis* 16M (A, B, F to I), or 1×10^3 CFU of *B. melitensis* 16M or mock infected with sterile PBS (sPBS) (C and D) and evaluated for ankle swelling over time (A and C). Mice were euthanized on day 14 postinfection, and joint and spleen bacterial loads were enumerated (B and D). (A) *, $P < 0.05$ compared to WT mice infected with 1×10^5 CFU of *B. melitensis* 16M. (C) *, $P < 0.05$ compared to mock-infected WT mice, and error bars depict standard errors of the mean. Representative plots of H&E-stained joint sections from mock-infected mice (E) or mice infected in the footpad with 1×10^5 CFU of *B. melitensis* 16M (F) 1×10^5 CFU of *B. suis* 1330 (G), 1×10^5 CFU of *B. abortus* 2308 (H), 1×10^4 CFU of *B. melitensis* 16M (I), or 1×10^3 CFU of *B. melitensis* 16M (J) are shown. Images (100×) are depicted with amplified boxed regions (400×) displayed beneath each image. Data from mice infected with 1×10^5 CFU of *B. melitensis* 16M is representative of 2 to 3 independent experiments, while data from other *Brucella* strains are representative of one experiment.

developed arthritis and musculoskeletal inflammation, while no pathology was evident in sterile PBS-inoculated animals (Fig. 2E). All mice infected with 1×10^5 CFU of *Brucella* spp. had a similar degree of neutrophil and macrophage infiltration in and around the joint space (Fig. 2F to H). Mice infected with lower doses of *B. melitensis* (Fig. 2I and J) also developed arthritis and musculoskeletal inflammation. While doses of 1×10^3 to 1×10^6 CFU all induced inflammation in this model, a dose of 1×10^6 was chosen for future studies as it was found to reliably generate detectable levels of joint cytokines in pilot studies (data not shown).

Adaptive immune responses mediate resolution of inflammation, but are not required for development of joint swelling. To investigate the role of adaptive immune responses during focal inflammation, C57BL/6 WT and Rag1$^{-/-}$ (B and T cell deficient) mice were infected in each hind footpad with 1×10^6 CFU of *B. melitensis* 16M, and ankle swelling was monitored for 30 days postinfection. At days 1 and 3 postinfection, both WT and Rag1$^{-/-}$ mice had developed a similar degree of ankle swelling; however, at days 6 and 8, Rag1$^{-/-}$ mice displayed a slight, but statistically significant, decrease in swelling compared to WT mice. After day 8, WT mice began to resolve joint swelling, but in Rag1$^{-/-}$ mice, swelling remained constant and was significantly greater than that in WT mice by day 27 postinfection (Fig. 3A). Joint *Brucella* loads in Rag1$^{-/-}$ mice were more than 1,000-fold greater than those in WT mice by day 30 postinfection (Fig. 3B). Joint inflammation was higher at day 30 in Rag1$^{-/-}$ mice relative to WT mice, and joint levels of the proinflammatory cytokines CXCL1, IL-1β, CCL2, and IL-6 were also significantly greater in Rag1$^{-/-}$ mice than WT mice (Fig. 3C to E). In addition, joints from WT mice had reduced amounts of fibrin relative to joints from Rag1$^{-/-}$ mice (Fig. 3E). These data demonstrate that adaptive immunity contributes to, but is not absolutely required for, the initiation of joint swelling and subsequently mediates bacterial clearance and resolution of joint inflammation.

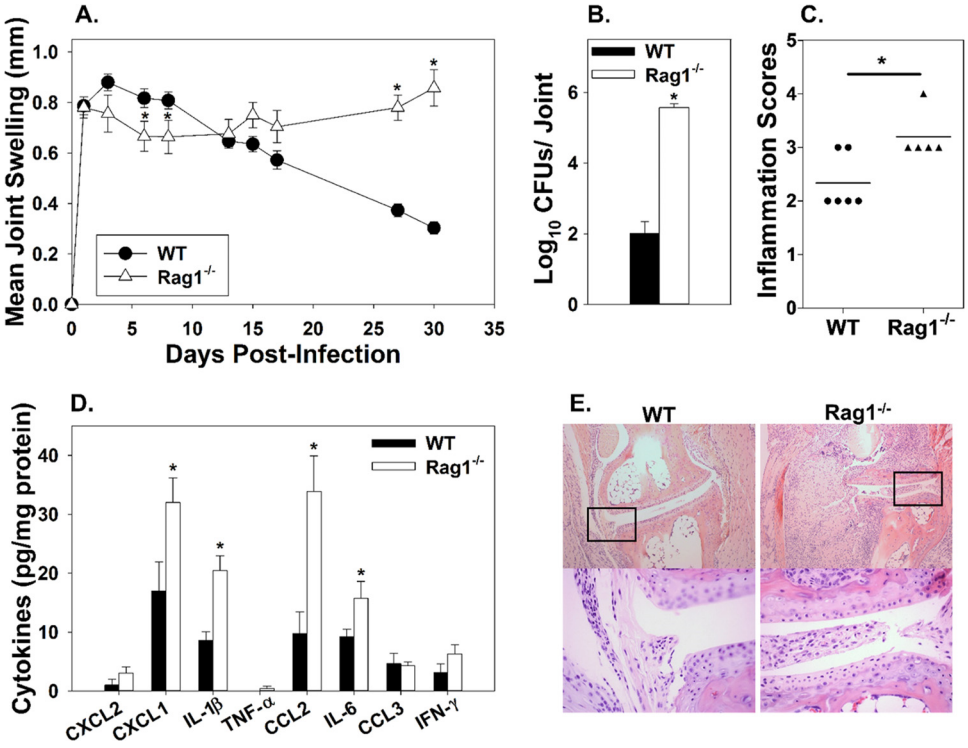

FIG 3 Adaptive immune responses are needed for inflammation resolution but not required for inflammation onset. C57BL/6 WT and Rag1$^{-/-}$ mice were infected in each rear footpad with 1×10^6 CFU of *B. melitensis* 16M. Joint swelling was recorded over time (5 to 10 mice/group) (A). Mice were euthanized at day 30 postinfection, and ankle joint bacterial loads ($n = 5$ to 10/group) (B) and cytokine levels ($n = 4$ to 5 mice/group) (D) were enumerated. H&E staining was conducted on joints at day 30 postinfection ($n = 5$ to 6/group) and scored for inflammation severity as follows: 0 = none (no inflammation), 1 = minimal with inflammation involving <5% of tissue, 2 = moderate with focally extensive areas of inflammation (5% to 25% of tissue and involving 1 or more tissues), 3 = moderate to severe with focally extensive areas of inflammation (>25% to 50% of tissue and involving multiple tissues), and 4 = severe with large confluent areas of inflammation (>50% of tissue and involving multiple tissues) (C). Representative images are depicted (100×), and amplified boxed regions are displayed beneath each image (400×) (E). *, $P < 0.05$ compared to WT mice. Error bars depict standard errors of the mean. Data are representative of one experiment.

MyD88 initiates early joint swelling, but is also required for clearance of *Brucella* from the joint and resolution of joint swelling. To determine if MyD88 was involved in the initiation of joint inflammation, swelling of C57BL/6 WT and MyD88$^{-/-}$ mouse ankles was measured over 28 days post-*Brucella*-infection. MyD88$^{-/-}$ mice infected with 1×10^6 CFU of *B. melitensis* 16M displayed reduced ankle swelling at days 1 and 3 postinfection (Fig. 4A). In contrast to the phenotype seen at days 1 and 3, MyD88$^{-/-}$ joints had increased swelling compared to WT joints by day 7 and at all subsequent time points postinfection (Fig. 4A). A similar effect of MyD88 on joint swelling was observed (albeit with delayed kinetics), when an infectious dose of 1×10^5 CFU was used (Fig. 4B).

To explain the increase in swelling of MyD88$^{-/-}$ joints after day 3 postinfection, we hypothesized that MyD88 is important for mediating bacterial clearance in the joint. Thus, bacterial loads were examined in ankle homogenates on days 1, 3, 7, 14, and 28 postinfection with 1×10^6 CFU of *B. melitensis* (Fig. 4C). While the numbers of joint CFU were similar between groups at day 1, by day 3, there were significantly greater bacterial loads in MyD88$^{-/-}$ joints compared to those in WT mice. This trend continued throughout the experimental time course (Fig. 4C).

MyD88 initiates early recruitment of inflammatory infiltrates following *B. melitensis* footpad infection. To assess the role of MyD88 in joint inflammation, H&E staining was conducted on C57BL/6 WT and MyD88$^{-/-}$ joints 3 days after infection with 1×10^6 CFU of *B. melitensis* 16M (Fig. 5A). Consistent with our swelling data,

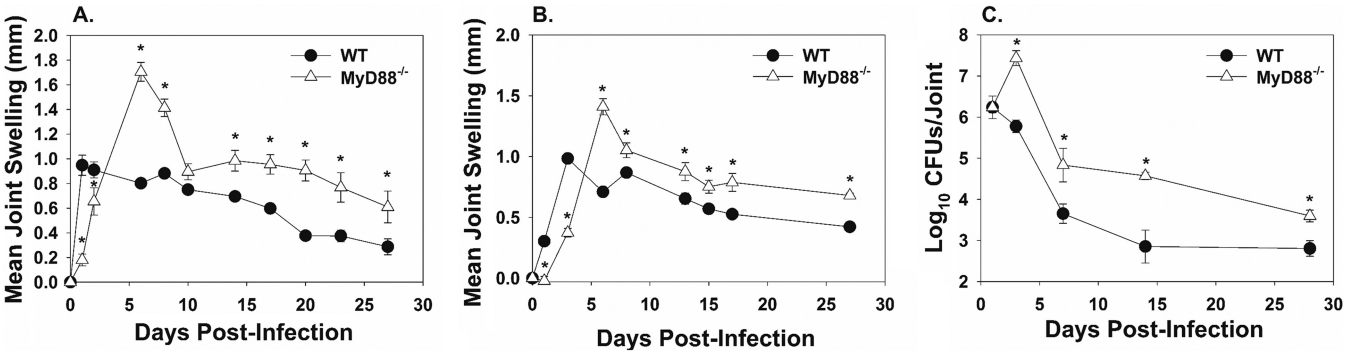

FIG 4 MyD88$^{-/-}$ mice have delayed joint swelling but increased joint *Brucella* burden. C57BL/6 WT and MyD88$^{-/-}$ mice were infected in each rear footpad with 1×10^6 (A) or 1×10^5 (B) CFU of *B. melitensis* 16M (4 to 5 mice/group), and swelling was recorded over time. At days 1, 3, 7, 14, and 28, mice infected with 1×10^6 CFU of *B. melitensis* were euthanized, and bacterial loads were enumerated in the ankle joint (3 to 4 mice/group/time point) (C). *, $P < 0.05$ compared to WT mice. Error bars depict standard errors of the mean. CFU data in panel C are from one kinetic experiment. Swelling curves are representative of two independent experiments.

MyD88$^{-/-}$ mice displayed visibly reduced inflammatory infiltrates, including macrophages and neutrophils (Fig. 5A). Inflammation severity scores of MyD88$^{-/-}$ joints at day 3 were significantly lower than those of infected WT mouse joints (Fig. 5B). Flow cytometry of infected joints also revealed reduced myeloid cell infiltration in MyD88$^{-/-}$ relative to WT joints early in infection (data not shown). Despite reduced inflammation at early time points, MyD88$^{-/-}$ mice developed similar pathology by day 7 and equaled or surpassed WT inflammation by days 14 and 28 postinfection (data not shown).

MyD88 mediates inflammatory cytokine production in *B. melitensis*-infected mouse joints early in infection. The production of inflammatory cytokines can induce inflammation and arthritis (33, 34). To determine which inflammatory cytokines are MyD88 dependent during *B. melitensis*-induced articular inflammation, cytokines were measured in ankle joint homogenates following footpad infection with 1×10^6 CFU of *B. melitensis* 16M. At day 1 postinfection, the concentrations of the proinflammatory cytokines CXCL2, CXCL1, IL-1β, tumor necrosis factor alpha (TNF-α), CCL2, IL-6, CCL3, and IFN-γ were all significantly lower in MyD88$^{-/-}$ compared to WT joint homogenates (Fig. 6A to H). However, by day 3 postinfection, TNF-α and IFN-γ concentrations in MyD88$^{-/-}$ joints increased to WT levels (Fig. 6D and H), while WT levels of CXCL1, CCL2, and IL-6 dropped and returned to similar levels to MyD88$^{-/-}$ joints (Fig. 6B, E, and F). At day 3 postinfection, IL-1β, CCL3, and CXCL2 levels increased in MyD88$^{-/-}$ joints, while WT levels decreased (Fig. 6A, C, and G). Eventually, all inflammatory cytokine concentrations became similar among groups by day 14 postinfection and at later time points.

MyD88 aids in systemic *Brucella* clearance and T cell production of IFN-γ. To determine if MyD88 is required for protection against systemic infection in this model, C57BL/6 WT and MyD88$^{-/-}$ mice were infected in the footpad with 1×10^6 CFU of *B. melitensis* 16M. *Brucella* spleen colonization in MyD88$^{-/-}$ mice was similar to that in WT mice until day 14; however, at 28 days postinfection, MyD88$^{-/-}$ mice had significantly increased splenic bacterial loads (Fig. 7A). To determine the role of MyD88 on systemic adaptive immune responses, CD4$^+$ and CD8$^+$ T cells from spleens of WT and MyD88$^{-/-}$ mice were evaluated for IFN-γ production. While the proportions of CD4$^+$ and CD8$^+$ T cells among splenocytes did not differ between WT and MyD88$^{-/-}$ mice (data not shown), at days 7 and 14 postinfection, the percentage of IFN-γ-producing CD4$^+$ and CD8$^+$ T cells was significantly lower in MyD88$^{-/-}$ mice than in WT mice (Fig. 7B and C). By day 28 postinfection, levels of IFN-γ production by T cells were similar between mouse strains (data not shown).

DISCUSSION

With over 500,000 human cases reported each year, brucellosis is a globally important zoonotic disease (35). Arthritis and musculoskeletal inflammation are the most

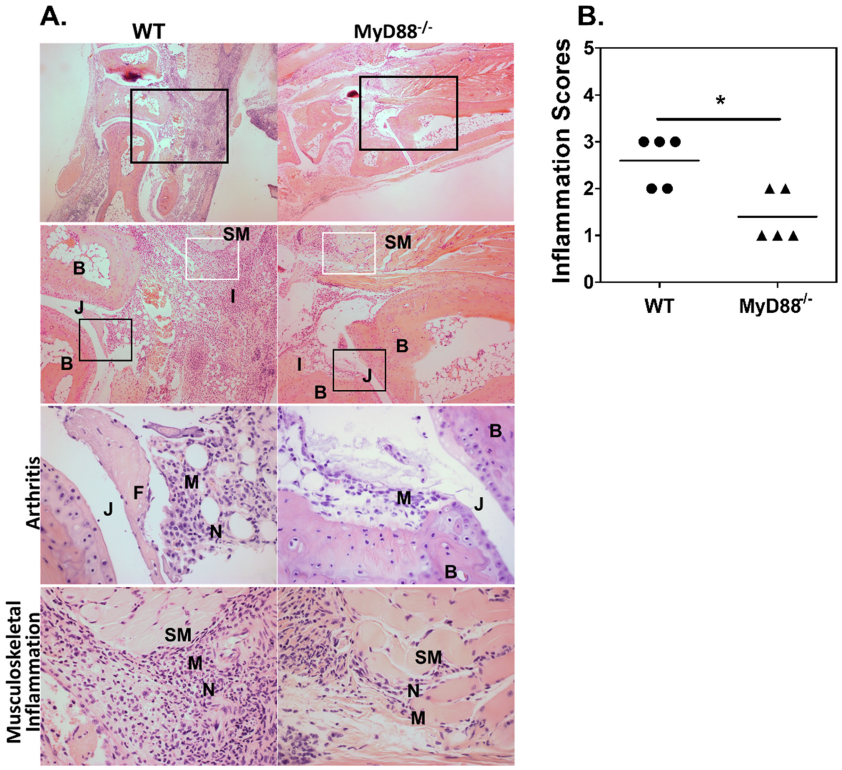

FIG 5 MyD88 mediates early arthritis and musculoskeletal inflammation. C57BL/6 WT and MyD88$^{-/-}$ mice were infected in each rear footpad with 1×10^6 CFU of *B. melitensis* 16M. Mice were euthanized 3 days postinfection, and H&E staining was conducted on mouse joints. Representative images of joint sections from WT and MyD88$^{-/-}$ mice are depicted with amplified boxed regions displayed beneath each image (A). Magnifications are as follows: row 1, 40×; row 2, 100×; rows 3 and 4, 400×. The black boxes indicate areas of arthritis or inflammation within and around the joint, and the white boxes indicate areas of musculoskeletal inflammation. Tissue architecture is indicated as follows: B, bone; SM, skeletal muscle; J, joint space. Areas of pathology are indicated as follows: I, inflammation; M, macrophages; N, neutrophils. Day 3 WT and MyD88$^{-/-}$ ankle joint H&E staining was scored for total inflammation as follows: 0 = none (no inflammation), 1 = minimal with inflammation involving <5% of tissue, 2 = moderate with focally extensive areas of inflammation (5% to 25% of tissue and involving 1 or more tissues), 3 = moderate to severe with focally extensive areas of inflammation (>25% to 50% of tissue and involving multiple tissues), 4 = severe with large confluent areas of inflammation (>50% of tissue and involving multiple tissues) (B). Histology scores are from one of two independent experiments (5 mice/group) from which sections were obtained. *, $P < 0.05$ compared to sections from WT mice.

common focal symptoms of human brucellosis (35, 36); however, the study of these manifestations has been hampered due to the absence of relevant mouse models. Intraperitoneal, pulmonary, or oral infection of wild-type, inbred mouse strains with conventional doses of *Brucella* does not induce arthritis and musculoskeletal inflammation. Others have demonstrated that intra-articular inoculation of heat-killed *Brucella* or *Brucella* lipoproteins into the knee induces osteoclastogenesis and recruitment of monocytes and neutrophils (37, 38). Footpad inoculation with *Brucella* spp. has been used to study *Brucella* dissemination and efficacy of vaccines (39–42), but inflammation in the joint and surrounding tissue was not described. Here we show that wild-type C57BL/6 mice inoculated via the footpad with 10^3 to 10^6 CFU of live *Brucella* develop arthritis and musculoskeletal inflammation. Similar to what has been described in human patients with articular brucellosis (14) and what we previously found in IFN-$\gamma^{-/-}$ mice, footpad-infected mice also developed inflammation of musculoskeletal tissues surrounding the joint. To our knowledge, this is the first description of a wild-type mouse strain developing arthritis and musculoskeletal inflammation when infected with a conventional dose of *Brucella*. We previously reported that IFN-$\gamma^{-/-}$ mice infected i.p. with *B. melitensis* developed exacerbated arthritis and joint colonization relative to IFN-$\gamma^{-/-}$ mice infected i.p. with *B. abortus* (9). However, here we

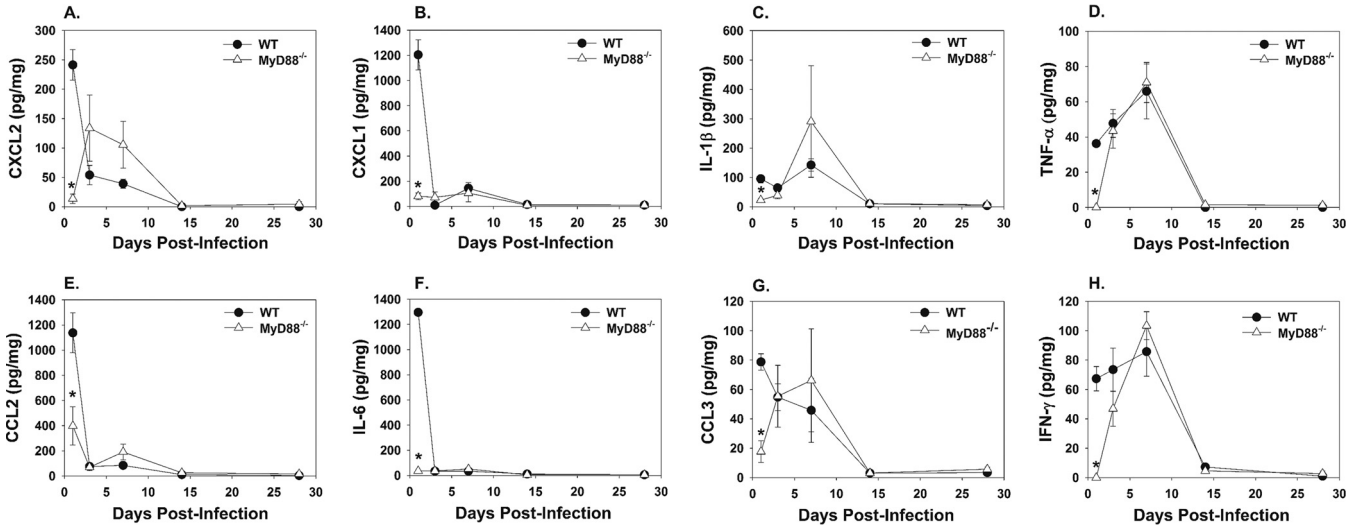

FIG 6 MyD88$^{-/-}$ joints have delayed cytokine production following footpad infection with *B. melitensis*. C57BL/6 WT and MyD88$^{-/-}$ mice (3 to 4 mice/group/time point) were infected in each rear footpad with 1×10^6 CFU of *B. melitensis* 16M and sacrificed at days 1, 3, 7, 14, and 28. Rear joints were homogenized, and CXCL2 (A), CXCL1 (B), IL-1β (C), TNF-α (D), CCL2 (E), IL-6 (F), CCL3 (G), and IFN-γ (H) concentrations were quantified by Luminex and normalized to total protein via BCA. *, $P < 0.05$ compared to infected WT mice. Error bars depict standard errors of the mean. Data are representative of one kinetic experiment.

found that following footpad inoculation, *B. melitensis*-, *B. abortus*-, and *B. suis*-infected mice all developed ankle swelling and exhibited similar joint bacterial loads and inflammation (Fig. 2A, B, and E to H). Thus, the augmented arthritogenicity of *B. melitensis* observed in IFN-$\gamma^{-/-}$ mice could be due to an enhanced ability to disseminate to the joint, rather than an enhanced ability to cause inflammation upon reaching

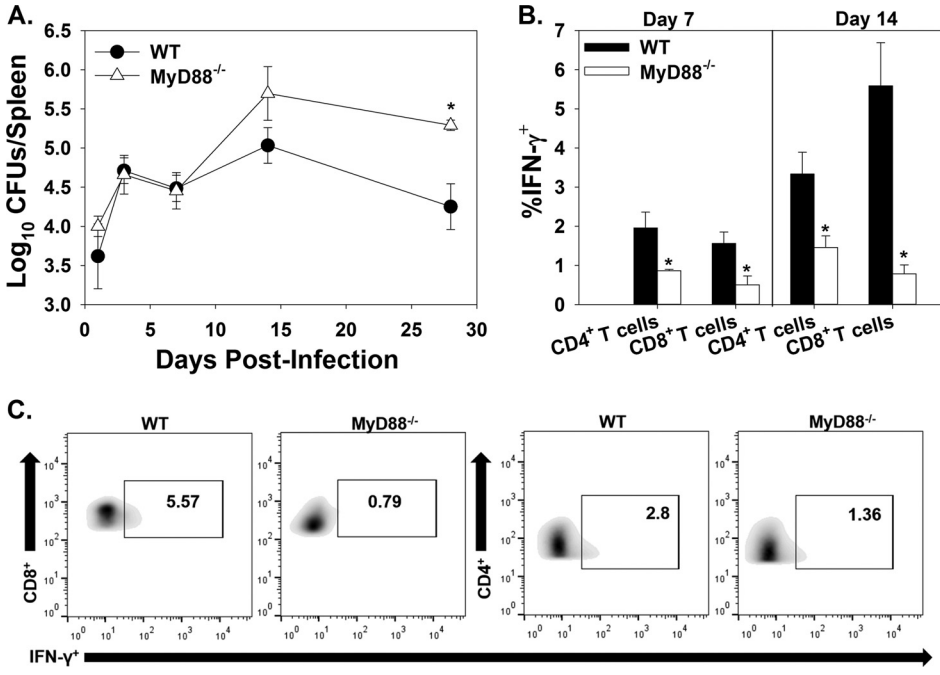

FIG 7 MyD88 aids in systemic *Brucella* clearance and T cell IFN-γ production. C57BL/6 WT and MyD88$^{-/-}$ mice were infected in each rear footpad with 1×10^6 CFU of *B. melitensis* 16M. At days 1, 3, 7, 14, and 28, mice were euthanized, and bacterial loads were enumerated in the spleen (3 to 4 mice/group/time point) (A). At days 7 and 14, flow cytometry was performed to determine IFN-γ production by T cells from infected mouse spleens (B). (C) Representative plots showing IFN-γ production by gated CD4$^+$ and CD8$^+$ T cells from WT and MyD88$^{-/-}$ mice 14 days postinfection. *, $P < 0.05$ compared to WT mice. Error bars depict standard errors of the mean. Data are representative of one kinetic experiment.

the joint. Similar to what we previously reported in i.p.-infected IFN-γ-deficient mice (17), here we found that adaptive immune responses are not required for joint swelling in footpad-inoculated mice. However, we did find that B and/or T cells are requisite for resolution of joint infection and inflammation in this model. Thus, resolution of infection and inflammation in the footpad model could be due to adaptive immune cell production of IFN-γ.

Utilizing this footpad model of *Brucella* infection, we demonstrated MyD88 is important for eliciting early inflammatory responses within the first 3 days postinfection. Aspects of MyD88-dependent inflammation appear to be protective at later times, as MyD88$^{-/-}$ mice had delayed resolution of inflammation. This may be due to increased bacterial loads as MyD88$^{-/-}$ mice had significantly higher joint bacterial burdens by day 3 postinfection compared to wild-type C57BL/6 mice. We also demonstrated that MyD88$^{-/-}$ mice had delayed expression of TNF-α, IL-1β, CCL2, IFN-γ, and CXCR2 ligands. This is of interest as these cytokines were found at elevated levels in the synovial fluid from a human brucellosis patient with arthritic manifestations (43). MyD88 has previously been shown to be important for controlling systemic *Brucella* infection in mice (44). Likewise, MyD88 signaling has been reported to drive dendritic cell maturation and in turn T cell secretion of IFN-γ, which is protective against systemic *Brucella* infection (45, 46). In this model, we demonstrated mice deficient in MyD88 have impaired CD8$^+$ and CD4$^+$ T cell production of IFN-γ in their spleens. This suggests the footpad model of *Brucella* infection may be a useful tool for analyzing systemic control of inflammation and *Brucella* clearance. Another *Brucella* infection model demonstrated macrophage and dendritic cell production of IL-12 and TNF-α are MyD88 dependent during systemic infection (45). TLR2 and TLR6 can recognize and protect against systemic brucellosis, and there is varied evidence that TLR4 may also be involved (28–31, 44, 47). TLR9 signaling can also increase the number of IFN-γ^+ cells after i.p. infection (47). Furthermore, IL-1 and IL-18 signaling can utilize MyD88 for downstream neutrophil recruitment, NK and T cell activation, and production of inflammatory cytokines (22, 23). Thus, the early inflammation and joint cytokine production mediated by MyD88 are likely due to TLR activation and/or IL-1R/IL-18R relay, which can contribute to *Brucella* clearance at later times.

Although MyD88 promotes inflammation early after infection, another mechanism independent of MyD88 induces inflammation by day 7. Joint levels of the inflammatory cytokines TNF-α, CXCL2, IL-1β, CCL3, and IFN-γ, in mice lacking MyD88 were elevated similarly to those in control animals by day 7, and swelling in MyD88$^{-/-}$ mouse joints was greater than that of control animals by day 6 postinfection. This increase in joint inflammation in MyD88$^{-/-}$ mice may also be dependent on damage-associated molecular patterns induced by overwhelming bacterial burden, which could signal through MyD88-independent pathways (48). It is becoming increasingly clear that cytosolic signaling mechanisms may also induce inflammation upon *Brucella* infection. Although the MyD88-independent inflammatory pathway has yet to be determined in this model, one study demonstrated an important role for inflammasomes that require the apoptosis-associated speck-like protein containing a caspase-recruitment domain (ASC) in the host response to *Brucella* infection (49). Additionally, neutrophils infected with *Brucella* have been shown to induce TAK1 and SYK kinase-dependent oxidative bursts (50). Thus, the inflammasome, TAK1-, and/or SYK kinase-dependent pathways could induce inflammation in mice lacking MyD88 in our model.

Although this is the first time MyD88 has been shown to be important for *Brucella* clearance in the joints, MyD88 is critical for joint pathogen clearance in *Borrelia burgdorferi*-induced arthritis. In contrast with *Brucella* infection, MyD88 does not appear to play a role in Lyme arthritis development (51, 52). In mice inoculated with *Escherichia coli* or *Streptococcus* cell wall fragments, MyD88 is critical for the induction of arthritis and is dependent on TLR2 and TLR4, respectively (26, 27). Similarly, TLR4 antagonism can suppress autoimmune arthritis models, such as collagen-induced arthritis (53). It is clear that MyD88 is responding to *Brucella* infection of the joints, but the nature of the reacting cell types remains unknown. Numerous cell types in the joint, including

macrophages, dendritic cells, synovial fibroblasts, chondrocytes, endothelial cells, and fibroblast-like synoviocytes, are capable of responding to exogenous and endogenous TLR ligands and could be mediating inflammation in our model (28, 54–58).

In summary, we have described a footpad model of *Brucella* infection that results in reproducible joint swelling, arthritis, and musculoskeletal inflammation following infection with *B. melitensis*, *B. abortus*, or *B. suis*. One aspect of human infection that this model does not recapitulate is the dissemination of *Brucella* to the joint. However, local delivery of *Brucella* directly to the joint and surrounding tissue allows us to synchronize infection and inflammation. This synchronization allows us to investigate mechanisms of the host response that are specific to these tissues, whereas in a systemic infection, deficiencies in the host immune response could affect bacterial dissemination to the joint and thus make it difficult to determine if changes in joint inflammation are due to local immune responses or due to a change in the dissemination of *Brucella* to the joint.

With this model, we are also able to study *Brucella*-induced arthritis in the context of an intact IFN-γ response. In IFN-γ-deficient mice, *Brucella*-induced focal inflammation does not resolve, and the animals eventually succumb to infection after 4 to 8 weeks. In this footpad infection model, mice do not display systemic symptoms of disease (beyond colonization of the spleen and liver) and are able to slowly resolve inflammation, an effect that requires adaptive immunity. Thus, this novel model allows us to study both the initiation and resolution of focal inflammation due to *Brucella* infection. Here we utilized this footpad model and determined MyD88-dependent pathways are responsible for induction of early arthritis and musculoskeletal inflammation; however, MyD88 deficiency also leads to an increase in joint bacterial loads, which may delay resolution of articular inflammation.

MATERIALS AND METHODS

Bacterial strains and growth conditions. All experiments with live *Brucella* cells were conducted in a biosafety level 3 (BSL3) facility at the University of Missouri. *B. melitensis* 16M and *B. abortus* 2308, obtained from Montana State University (Bozeman, MT), and *B. suis* 1330, obtained from BEI Resources (Manassas, VA), were grown for 3 days at 37°C in 5% CO_2 on brucella agar (Becton Dickinson). Colonies were picked from brucella agar and grown overnight in brucella broth (Becton Dickinson) at 37°C while shaking. The *Brucella* inoculum was prepared by estimating the concentration of bacteria by measuring optical density at 600 nm and diluting to the appropriate concentration in sterile phosphate-buffered saline (sPBS). Viable titers of inoculum were verified by serial dilutions of *Brucella* onto brucella agar.

Mice. Experiments were conducted using 6- to 10-week-old age- and sex-matched mice on a C57BL/6 background. C57BL/6 Rag1$^{-/-}$ mice and breeding pairs of MyD88$^{-/-}$ mice were obtained from the Jackson Laboratory (Bar Harbor, ME). Mice were infected in both rear footpads with a volume of 50 μl containing ~1 × 10^3, 1 × 10^4, 1 × 10^5, or 1 × 10^6 CFU of *Brucella*. After infection, all mice were maintained in individually ventilated cages under high-efficiency particulate air-filtered barrier conditions of 12 h of light and 12 h of darkness in animal BSL3 facilities and were provided with sterile food and water. All studies were conducted in accordance with University of Missouri Animal Care and Use Committee guidelines.

Bacterial burdens. At various times after infection, mice were euthanized, and spleens and rear mouse paws (following skin removal) were harvested. Spleens and paws were homogenized mechanically in sPBS. A series of 10-fold serial dilutions were performed in triplicate in sPBS and plated onto brucella agar. Plates were incubated 3 to 6 days at 37°C, colonies were enumerated, and the number of CFU per tissue was determined.

Assessment of pathology. Ankle swelling was measured at various time points by collective measurements of both rear tibiotarsal joints. Basal joint measurements were made prior to infection, and the difference was used to calculate mean joint swelling. For histology of mouse ankles, skin was removed, and ankles were fixed in 10% buffered zinc formalin, decalcified in 15% formic acid, rinsed in tap water, and dehydrated with an alcohol gradient and clearing agent. Tissue specimens were embedded in paraffin. Tissue sections (5 μm) were mounted on glass slides, and serial sections were stained with hematoxylin and eosin (H&E) and covered by a coverslip with aqueous mounting medium. Sections were evaluated for inflammation, which involved multiple tissues (joint, bone, tendons, skeletal muscle, and skin). Two sections of ankle (bone and associated structures) were evaluated for each mouse. Sections were evaluated by histopathology and scored for lesion severity (inflammation) in a blinded manner by an experienced pathologist. The following scale was used: 0 = none (no inflammation); 1 = minimal with inflammation involving <5% of tissue; 2 = moderate with focally extensive areas of inflammation (5% to 25% of tissue and involving 1 or more tissues); 3 = moderate to severe with focally extensive areas of inflammation (>25% to 50% of tissue and involving multiple tissues); and 4 = severe with large confluent areas of inflammation (>50% of tissue and involving multiple tissues).

Flow cytometry. Spleens were homogenized in 900 μl of sterile PBS. Tissue homogenates were strained through an 80-μm-pore mesh and washed with complete medium (CM: RPMI 1640, 0.1 HEPES,

1 mM sodium pyruvate, 1 mM nonessential amino acids, and 10% fetal bovine serum [FBS]) Cells were resuspended in RPMI medium with 0.1 mM HEPES, and red blood cells were lysed. Spleen cells were then washed and resuspended in CM and cultured for 4 h at 37°C in 5% CO_2 with a cell stimulation cocktail containing phorbol 12-myristate 13-acetate (PMA), ionomycin, brefeldin A, and monensin (Ebioscience). Cells were then stained for surface markers (anti-CD4, clone GK1.5; anti-CD8, clone 2.43) and fixed in paraformaldehyde. Cells were permeabilized with 0.2% saponin prior to intracellular staining for IFN-γ (clone XMG1.2). Fluorescence was acquired on a CyAn ADP analyzer (Beckman Coulter), and FlowJo (Tree Star) software was used for analysis.

Ankle processing and cytokine measurements. Following skin removal, ankles from each mouse were excised, combined, and then homogenized *in toto* in 3 to 4 ml of sPBS treated with Halt protease inhibitor cocktail (Thermo Scientific). Homogenized tissues were then centrifuged at 2,000 × *g* for 5 min, and supernatants were filter sterilized (0.2-μm pore) and stored at −70°C until analysis using a Luminex MagPix instrument with Milliplex magnetic reagents according to the manufacturer's instructions (Millipore). Luminex data were analyzed with Milliplex Analyst software (Millipore) and normalized to total protein levels determined by a bicinchoninic acid (BCA) protein assay (Thermo Scientific).

Statistical analysis. Statistical analysis of the difference between 2 mean values was conducted using the Student *t* test with significance set at $P \leq 0.05$, while comparisons of ≥3 mean values was done using analysis of variance (ANOVA), followed by the Dunnett's test. The statistical significance of differences in histology scores was determined by a one-tailed Mann-Whitney U test.

ACKNOWLEDGMENTS

This work was supported by NIH/National Institute of Allergy and Infectious Diseases grant 1R21AI119634 to J.A.S. and funds from the University of Missouri College of Veterinary Medicine and Research Board.

The authors do not have a commercial or other association that might pose a conflict of interest.

REFERENCES

1. Colmenero JD, Reguera JM, Fernandez-Nebro A, Cabrera-Franquelo F. 1991. Osteoarticular complications of brucellosis. Ann Rheum Dis 50:23–26. https://doi.org/10.1136/ard.50.1.23.
2. Anonymous. 2012. Research priorities for zoonoses and marginalized infections. World Health Organ Tech Rep Ser 2012:ix–xi, 1–119, 2 p following p 119.
3. Zinsstag J, Roth F, Orkhon D, Chimed-Ochir G, Nansalmaa M, Kolar J, Vounatsou P. 2005. A model of animal-human brucellosis transmission in Mongolia. Prev Vet Med 69:77–95. https://doi.org/10.1016/j.prevetmed.2005.01.017.
4. Kaufmann AF, Fox MD, Boyce JM, Anderson DC, Potter ME, Martone WJ, Patton CM. 1980. Airborne spread of brucellosis. Ann N Y Acad Sci 353:105–114. https://doi.org/10.1111/j.1749-6632.1980.tb18912.x.
5. Mableson HE, Okello A, Picozzi K, Welburn SC. 2014. Neglected zoonotic diseases—the long and winding road to advocacy. PLoS Negl Trop Dis 8:e2800. https://doi.org/10.1371/journal.pntd.0002800.
6. Roth F, Zinsstag J, Orkhon D, Chimed-Ochir G, Hutton G, Cosivi O, Carrin G, Otte J. 2003. Human health benefits from livestock vaccination for brucellosis: case study. Bull World Health Organ 81:867–876.
7. Rajapakse CN. 1995. Bacterial infections: osteoarticular brucellosis. Bailliere's Clin Rheumatol 9:161–177. https://doi.org/10.1016/S0950-3579(05)80153-0.
8. Gotuzzo E, Alarcon GS, Bocanegra TS, Carrillo C, Guerra JC, Rolando I, Espinoza LR. 1982. Articular involvement in human brucellosis: a retrospective analysis of 304 cases. Semin Arthritis Rheum 12:245–255. https://doi.org/10.1016/0049-0172(82)90064-6.
9. Skyberg JA, Thornburg T, Kochetkova I, Layton W, Callis G, Rollins MF, Riccardi C, Becker T, Golden S, Pascual DW. 2012. IFN-γ-deficient mice develop IL-1-dependent cutaneous and musculoskeletal inflammation during experimental brucellosis. J Leukoc Biol 92:375–387. https://doi.org/10.1189/jlb.1211626.
10. Yagupsky P, Peled N. 2002. Use of the Isolator 1.5 microbial tube for detection of *Brucella melitensis* in synovial fluid. J Clin Microbiol 40:3878. https://doi.org/10.1128/JCM.40.10.3878.2002.
11. Shaalan MA, Memish ZA, Mahmoud SA, Alomari A, Khan MY, Almuneef M, Alalola S. 2002. Brucellosis in children: clinical observations in 115 cases. Int J Infect Dis 6:182–186. https://doi.org/10.1016/S1201-9712(02)90108-6.
12. al-Eissa YA, Kambal AM, Alrabeeah AA, Abdullah AM, al-Jurayyan NA, al-Jishi NM. 1990. Osteoarticular brucellosis in children. Ann Rheum Dis 49:896–900. https://doi.org/10.1136/ard.49.11.896.
13. Madkour MM. 1989. Bone and joint brucellosis, p 90–104. Brucellosis. Butterworths, London, United Kingdom.
14. Ayaşlıoğlu E, Özlük Ö, Kılıç D, Kaygusuz S, Kara S, Aydın G, Çokca F, Tekeli E. 2005. A case of brucellar septic arthritis of the knee with a prolonged clinical course. Rheumatol Int 25:69–71. https://doi.org/10.1007/s00296-004-0453-1.
15. Laajam MA. 1985. Synovial rupture complicating *Brucella* arthritis. Br J Rheumatol 24:191–193. https://doi.org/10.1093/rheumatology/24.2.191.
16. Kelly PJ, Martin WJ, Schirger A, Weed LA. 1960. Brucellosis of the bones and joints: experience with thirty-six patients. JAMA 174:347–353. https://doi.org/10.1001/jama.1960.03030040001001.
17. Lacey CA, Keleher LL, Mitchell WJ, Brown CR, Skyberg JA. 2016. CXCR2 mediates *Brucella*-induced arthritis in interferon gamma-deficient mice. J Infect Dis 214:151–160. https://doi.org/10.1093/infdis/jiw087.
18. Magnani DM, Lyons ET, Forde TS, Shekhani MT, Adarichev VA, Splitter GA. 2013. Osteoarticular tissue infection and development of skeletal pathology in murine brucellosis. Dis Model Mech 6:811–818. https://doi.org/10.1242/dmm.011056.
19. Morrison TE, Oko L, Montgomery SA, Whitmore AC, Lotstein AR, Gunn BM, Elmore SA, Heise MT. 2011. A mouse model of chikungunya virus-induced musculoskeletal inflammatory disease: evidence of arthritis, tenosynovitis, myositis, and persistence. Am J Pathol 178:32–40. https://doi.org/10.1016/j.ajpath.2010.11.018.
20. Lee JH. 2011. Involvement of T-cell immunoregulation by ochnaflavone in therapeutic effect on fungal arthritis due to *Candida albicans*. Arch Pharm Res 34:1209–1217. https://doi.org/10.1007/s12272-011-0720-0.
21. Brown CR, Reiner SL. 1999. Genetic control of experimental Lyme arthritis in the absence of specific immunity. Infect Immun 67:1967–1973.
22. Adachi O, Kawai T, Takeda K, Matsumoto M, Tsutsui H, Sakagami M, Nakanishi K, Akira S. 1998. Targeted disruption of the MyD88 gene results in loss of IL-1- and IL-18-mediated function. Immunity 9:143–150. https://doi.org/10.1016/S1074-7613(00)80596-8.
23. Miller LS, O'Connell RM, Gutierrez MA, Pietras EM, Shahangian A, Gross CE, Thirumala A, Cheung AL, Cheng G, Modlin RL. 2006. MyD88 mediates neutrophil recruitment initiated by IL-1R but not TLR2 activation in immunity against *Staphylococcus aureus*. Immunity 24:79–91. https://doi.org/10.1016/j.immuni.2005.11.011.
24. Kawai T, Akira S. 2005. Toll-like receptor downstream signaling. Arthritis Res Ther 7:12–19. https://doi.org/10.1186/ar1469.
25. Chen Z, Su L, Xu Q, Katz J, Michalek SM, Fan M, Feng X, Zhang P. 2015. IL-1R/TLR2 through MyD88 divergently modulates osteoclastogenesis

through regulation of nuclear factor of activated T cells c1 (NFATc1) and B lymphocyte-induced maturation protein-1 (Blimp1). J Biol Chem 290: 30163–30174. https://doi.org/10.1074/jbc.M115.663518.
26. Kyo F, Futani H, Matsui K, Terada M, Adachi K, Nagata K, Sano H, Tateishi H, Tsutsui H, Nakanishi K. 2005. Endogenous interleukin-6, but not tumor necrosis factor α, contributes to the development of Toll-like receptor 4/myeloid differentiation factor 88-mediated acute arthritis in mice. Arthritis Rheumatol 52:2530–2540. https://doi.org/10.1002/art.21213.
27. Joosten LA, Koenders MI, Smeets RL, Heuvelmans-Jacobs M, Helsen MM, Takeda K, Akira S, Lubberts E, van de Loo FA, van den Berg WB. 2003. Toll-like receptor 2 pathway drives streptococcal cell wall-induced joint inflammation: critical role of myeloid differentiation factor 88. J Immunol 171:6145–6153. https://doi.org/10.4049/jimmunol.171.11.6145.
28. Gomes MT, Campos PC, Pereira Gde S, Bartholomeu DC, Splitter G, Oliveira SC. 2016. TLR9 is required for MAPK/NF-kappaB activation but does not cooperate with TLR2 or TLR6 to induce host resistance to *Brucella abortus*. J Leukoc Biol 99:771–780. https://doi.org/10.1189/jlb.4A0815-346R.
29. Ferrero MC, Hielpos MS, Carvalho NB, Barrionuevo P, Corsetti PP, Giambartolomei GH, Oliveira SC, Baldi PC. 2014. Key role of Toll-like receptor 2 in the inflammatory response and major histocompatibility complex class II downregulation in *Brucella abortus*-infected alveolar macrophages. Infect Immun 82:626–639. https://doi.org/10.1128/IAI.01237-13.
30. de Almeida LA, Macedo GC, Marinho FA, Gomes MT, Corsetti PP, Silva AM, Cassataro J, Giambartolomei GH, Oliveira SC. 2013. Toll-like receptor 6 plays an important role in host innate resistance to *Brucella abortus* infection in mice. Infect Immun 81:1654–1662. https://doi.org/10.1128/IAI.01356-12.
31. Campos MA, Rosinha GM, Almeida IC, Salgueiro XS, Jarvis BW, Splitter GA, Qureshi N, Bruna-Romero O, Gazzinelli RT, Oliveira SC. 2004. Role of Toll-like receptor 4 in induction of cell-mediated immunity and resistance to *Brucella abortus* infection in mice. Infect Immun 72:176–186. https://doi.org/10.1128/IAI.72.1.176-186.2004.
32. Vieira ALS, Silva TM, Mol JP, Oliveira SC, Santos RL, Paixão TA. 2013. MyD88 and TLR9 are required for early control of *Brucella ovis* infection in mice. Res Vet Sci 94:399–405. https://doi.org/10.1016/j.rvsc.2012.10.028.
33. Isomäki P, Punnonen J. 1997. Pro- and anti-inflammatory cytokines in rheumatoid arthritis. Ann Med 29:499–507. https://doi.org/10.3109/07853899709007474.
34. Tarkowski A. 2006. Infectious arthritis. Best Pract Res Clin Rheumatol 20:1029–1044. https://doi.org/10.1016/j.berh.2006.08.001.
35. Pappas G, Papadimitriou P, Akritidis N, Christou L, Tsianos EV. 2006. The new global map of human brucellosis. Lancet Infect Dis 6:91–99. https://doi.org/10.1016/S1473-3099(06)70382-6.
36. Young EJ. 1995. An overview of human brucellosis. Clin Infect Dis 21:283–289. https://doi.org/10.1093/clinids/21.2.283.
37. Delpino MV, Barrionuevo P, Macedo GC, Oliveira SC, Genaro SD, Scian R, Miraglia MC, Fossati CA, Baldi PC, Giambartolomei GH. 2012. Macrophage-elicited osteoclastogenesis in response to *Brucella abortus* infection requires TLR2/MyD88-dependent TNF-alpha production. J Leukoc Biol 91:285–298. https://doi.org/10.1189/jlb.04111185.
38. Scian R, Barrionuevo P, Giambartolomei GH, De Simone EA, Vanzulli SI, Fossati CA, Baldi PC, Delpino MV. 2011. Potential role of fibroblast-like synoviocytes in joint damage induced by *Brucella abortus* infection through production and induction of matrix metalloproteinases. Infect Immun 79:3619–3632. https://doi.org/10.1128/IAI.05408-11.
39. Bosseray N. 1980. Colonization of mouse placentas by *Brucella abortus* inoculated during pregnancy. Br J Exp Pathol 61:361–368.
40. Bosseray N, Plommet M. 1990. *Brucella suis* S2, *Brucella melitensis* Rev.1 and *Brucella abortus* S19 living vaccines: residual virulence and immunity induced against three *Brucella* species challenge strains in mice. Vaccine 8:462–468. https://doi.org/10.1016/0264-410X(90)90247-J.
41. Plommet M, Plommet A-M. 1983. Immune serum-mediated effects on brucellosis evolution in mice. Infect Immun 41:97–105.
42. Pardon P. 1977. Resistance against a subcutaneous *Brucella* challenge of mice immunized with living or dead *Brucella* or by transfer of immune serum. Ann Immunol (Paris) 128:1025–1037.
43. Wallach JC, Delpino MV, Scian R, Deodato B, Fossati CA, Baldi PC. 2010. Prepatellar bursitis due to *Brucella abortus*: case report and analysis of the local immune response. J Med Microbiol 59:1514–1518. https://doi.org/10.1099/jmm.0.016360-0.
44. Weiss DS, Takeda K, Akira S, Zychlinsky A, Moreno E. 2005. MyD88, but not Toll-like receptors 4 and 2, is required for efficient clearance of *Brucella abortus*. Infect Immun 73:5137–5143. https://doi.org/10.1128/IAI.73.8.5137-5143.2005.
45. Macedo GC, Magnani DM, Carvalho NB, Bruna-Romero O, Gazzinelli RT, Oliveira SC. 2008. Central role of MyD88-dependent dendritic cell maturation and proinflammatory cytokine production to control *Brucella abortus* infection. J Immunol 180:1080–1087. https://doi.org/10.4049/jimmunol.180.2.1080.
46. Murphy EA, Sathiyaseelan J, Parent MA, Zou B, Baldwin CL. 2001. Interferon-γ is crucial for surviving a *Brucella abortus* infection in both resistant C57BL/6 and susceptible BALB/c mice. Immunology 103: 511–518. https://doi.org/10.1046/j.1365-2567.2001.01258.x.
47. Copin R, De Baetselier P, Carlier Y, Letesson JJ, Muraille E. 2007. MyD88-dependent activation of B220-CD11b$^+$ LY-6C$^+$ dendritic cells during *Brucella melitensis* infection. J Immunol 178:5182–5191. https://doi.org/10.4049/jimmunol.178.8.5182.
48. Foell D, Wittkowski H, Roth J. 2007. Mechanisms of disease: a 'DAMP' view of inflammatory arthritis. Nat Clin Pract Rheumatol 3:382–390.
49. Gomes MT, Campos PC, Oliveira FS, Corsetti PP, Bortoluci KR, Cunha LD, Zamboni DS, Oliveira SC. 2013. Critical role of ASC inflammasomes and bacterial type IV secretion system in caspase-1 activation and host innate resistance to *Brucella abortus* infection. J Immunol 190: 3629–3638. https://doi.org/10.4049/jimmunol.1202817.
50. Keleher LL, Skyberg JA. 2016. Activation of bovine neutrophils by *Brucella* spp. Vet Immunol Immunopathol 177:1–6. https://doi.org/10.1016/j.vetimm.2016.05.011.
51. Liu N, Montgomery RR, Barthold SW, Bockenstedt LK. 2004. Myeloid differentiation antigen 88 deficiency impairs pathogen clearance but does not alter inflammation in *Borrelia burgdorferi*-infected mice. Infect Immun 72:3195–3203. https://doi.org/10.1128/IAI.72.6.3195-3203.2004.
52. Bolz DD, Sundsbak RS, Ma Y, Akira S, Kirschning CJ, Zachary JF, Weis JH, Weis JJ. 2004. MyD88 plays a unique role in host defense but not arthritis development in Lyme disease. J Immunol 173:2003–2010. https://doi.org/10.4049/jimmunol.173.3.2003.
53. Abdollahi-Roodsaz S, Joosten LA, Roelofs MF, Radstake TR, Matera G, Popa C, van der Meer JW, Netea MG, van den Berg WB. 2007. Inhibition of Toll-like receptor 4 breaks the inflammatory loop in autoimmune destructive arthritis. Arthritis Rheum 56:2957–2967. https://doi.org/10.1002/art.22848.
54. Delpino MV, Fossati CA, Baldi PC. 2009. Proinflammatory response of human osteoblastic cell lines and osteoblast-monocyte interaction upon infection with *Brucella* spp. Infect Immun 77:984–995. https://doi.org/10.1128/IAI.01259-08.
55. Surendran N, Hiltbold EM, Heid B, Akira S, Standiford TJ, Sriranganathan N, Boyle SM, Zimmerman KL, Makris MR, Witonsky SG. 2012. Role of TLRs in *Brucella* mediated murine DC activation in vitro and clearance of pulmonary infection in vivo. Vaccine 30:1502–1512. https://doi.org/10.1016/j.vaccine.2011.12.036.
56. Scian R, Barrionuevo P, Rodriguez AM, Arriola Benitez PC, Garcia Samartino C, Fossati CA, Giambartolomei GH, Delpino MV. 2013. *Brucella abortus* invasion of synoviocytes inhibits apoptosis and induces bone resorption through RANKL expression. Infect Immun 81:1940–1951. https://doi.org/10.1128/IAI.01366-12.
57. Nair A, Kanda V, Bush-Joseph C, Verma N, Chubinskaya S, Mikecz K, Glant TT, Malfait AM, Crow MK, Spear GT, Finnegan A, Scanzello CR. 2012. Synovial fluid from patients with early osteoarthritis modulates fibroblast-like synoviocyte responses to Toll-like receptor 4 and Toll-like receptor 2 ligands via soluble CD14. Arthritis Rheum 64:2268–2277. https://doi.org/10.1002/art.34495.
58. Liu-Bryan R, Pritzker K, Firestein GS, Terkeltaub R. 2005. TLR2 signaling in chondrocytes drives calcium pyrophosphate dihydrate and monosodium urate crystal-induced nitric oxide generation. J Immunol 174: 5016–5023. https://doi.org/10.4049/jimmunol.174.8.5016.